Program Digest, 2019 IEEE International Ultrasonics Symposium (IUS)
Glasgow, Scotland, October 6-9, 2019

Reflection-mode speed-of-sound imaging using soft-prior limits

1st Patrick Stähli
Institute of Applied Physics
Unversity of Bern
Bern, Switzerland
patrick.staehli@iap.unibe.ch

2nd Martin Frenz
Institute of Applied Physics
Unversity of Bern
Bern, Switzerland
martin.frenz@iap.unibe.ch

3rd Michael Jaeger
Institute of Applied Physics
Unversity of Bern
Bern, Switzerland
michael.jaeger@iap.unibe.ch

***Abstract*—The diagnostic accuracy of classical gray-scale ultrasound (US) can be improved by complementing with new multimodal information. One promising candidate is speed-of-sound (SOS) imaging that reveals disease-related changes of tissue composition and structure. Computed ultrasound tomography in echo mode (CUTE) determines the spatial distribution of SoS based on pulse-echo signals by measuring the changing phase of an echo that is detected under a variety of transmit/receive settings. The SoS is then reconstructed via a regularized inversion of a forward model linking the SoS to the echo phase shift. In-vivo, clutter and aberration lead to phase noise that causes strong artefacts in the reconstructed SoS when using the previously proposed regularization of the spatial gradient of SoS (SG). To solve this shortcoming, we propose a soft-prior (SP) regularization that includes a statistical *a priori* description of the samples mean SoS variability of SoS. Both regularization approaches are compared in a phantom study mimicking the abdominal wall and liver tissue, where the SP regularization proves a much higher stability against phase noise. In an in-vivo scenario imaging a volunteer's liver, only the SP regularization leads to reproducible SoS reconstructions of the liver's SoS independent, of the scanning location.**

***Index Terms*—Ultrasound tomography, pulse-echo ultrasound, regularization**

I. Introduction

Medical ultrasound (US) is routinely used in radiology for various different diagnostic applications. Conventional B-mode US displays the tissue's echogenicity in a spatially resolved way, allowing the evaluation of various traumatic and pathologic conditions. However, not every disease type influences the echogenicity. Together with the natural variability of healthy tissue, this leads to difficulties of B-mode US in differential diagnosis of certain disease types. Disease progression is often reflected by changes of mechanical properties of the tissue composition. Imaging these properties in a multimodal approach may complement B-mode US with additional structural and functional information to improve the detection of tissue abnormalities. For this reason, various approaches have been proposed to determine the speed-of-sound (SoS) inside tissue in reflection mode. We have recently developed computed ultrasound tomography in echo mode (CUTE) for handheld imaging of the spatial distribution of SoS inside tissue in real time with promising spatial and contrast resolution [1] [2]. The working principle of CUTE is straightforward: Radio-frequency (RF) mode US images are beamformed (using e.g. conventional delay-and-sum algorithm) under a set of various different transmit (Tx) and receive (Rx) angles. Successively, maps of local echo-phase shift are determined between different combinations of Tx and Rx angles. The SoS is finally reconstructed by inverting a forward model describing the relation of the spatial distribution of echo-phase shift and the spatial distribution of the SoS [2]. This inverse problem is ill-posed and thus requires some way of regularization. Promising results were achieved in phantoms using a Tikhonov regularization of the spatial gradient (SG) of SoS [2] [3]. In-vivo, however, clutter and aberration leads to an increased phase noise. In many subjects this phase noise is that strong that the SG regularization leads to artificial SoS variations within tissue regions where the SoS is known to be uniform. To solve this shortcoming, we propose a soft-prior (SP) regularization, inspired by results obtained in near-infrared optical tomography [4] [5]. In contrary to the blind SG regularization, the SP approach aims at a regularization that is optimised under an *a priori* statistical description of the variability of the SoS distribution. This allows to include ad hoc knowledge of the position of tissue boundaries where properties – in our case SoS – are known to vary on a short spatial scale. In this study, we derive the position of tissue boundaries from segmentation of B-mode US images that are acquired in parallel to CUTE, and we compare the performance of SG and SP regularization in a phantom and in-vivo study.

This research has received funding in part from the Swiss National Science Foundation (No. 205320_179038/1), from the European Union's Horizon 2020 research and innovation programme under grant agreement No 731771, and from the Photonics Private Public Partnership, and is supported by the Swiss State Secretariat for Education, Research and Innovation (SERI) under contract number 16.0160. The opinions expressed and arguments employed herein do not necessarily reflect the official view of the Swiss Government.

II. Methodology

Plane-wave pulse-echo RF data were acquired and beamformed (using delay-and-sum together with coherent plane-wave compounding), for a set of transmit (Tx) and receive (Rx) angles ranging from $-25°$ to $25°$ deg in $2°$ steps. Using Loupas phase correlation [6], the local echo-phase shift was successively determined over the set of Tx and Rx angles

following the common-mid-angle approach outlined in [2]. The phase shift maps are related to the slowness (inverse SoS) distribution via a forward model [2]. Assuming the straight-ray approximation of sound propagation, the forward model can be formulated in matrix notation:

$$\Delta\Theta = \mathbf{M}\Delta s + \epsilon \tag{1}$$

$\Delta\Theta$ represents the vectorized phase shift maps, Δs the vectorized distribution of the difference between the actual slowness and the reference slowness that was used for beamforming. The forward model is encoded in the matrix $\mathbf{M}$ and ϵ describes the measurement noise that contaminates the echo-phase shift maps.

A. Image reconstruction using spatial gradient regularization

Since $\mathbf{M}$ is poorly-conditioned and $\Delta\Theta$ steadily contaminated by noise, (1) is not expected to have an exact solution. Instead, an objective function $C(\Delta s)$ is defined that describes to what extent Δs matches $\Delta\Theta$, via the squared L2 norm of the residuals:

$$C(\mathbf{\Delta s}) = \|\Delta\Theta - \mathbf{M}\Delta s\|_2^2 + \gamma^2\|\mathbf{D}\Delta s\|_2^2 \tag{2}$$

The second term on the right-hand side is the regularization term. Regularization prevents (2) to be unduly sensitive to noise-level variations in the data vector. γ is a positive regularization parameter and $\mathbf{D}$ a pre-determined matrix. One then can show that the estimated slowness deviation $\widehat{\Delta s}$ is:

$$\widehat{\Delta s} = \left(\mathbf{M}^T\mathbf{M} + \gamma\mathbf{D}^T\mathbf{D}\right)^{\text{inv}}\mathbf{M}^T\Delta\Theta \tag{3}$$

Finally, the SoS is recovered from the estimated slowness deviation $\widehat{\Delta s}$. In previous studies, the regularization matrix $\mathbf{D}$ was chosen as finite difference operators in x and z direction with independent regularization parameters γ_x and γ_y:

$$\gamma\mathbf{D}^T\mathbf{D} = \gamma_x\mathbf{D}_\mathbf{x}^\mathbf{T}\mathbf{D}_\mathbf{x} + \gamma_z\mathbf{D}_\mathbf{z}^\mathbf{T}\mathbf{D}_\mathbf{z} \tag{4}$$

The finite difference regularization enforces a smooth slowness profile of the to-be reconstructed slowness. A large regularization parameter therefore forces a uniform slowness distribution in the to-be reconstructed slowness image but also decreases the contrast resolution of the image.

B. Encoding spatial soft-prior information

A parameter estimation of Δs can also be derived based on a Bayesian interpretation [7] [8]. In the Bayesian analysis, a specific *a priori* probabilistic distribution over the model space of possible solutions Δs is involved, assuming that this distribution is Gaussian in form, centered upon a mean (per-pixel) value Δs_p with a (inter-pixel) covariance matrix $\mathbf{C}_{\Delta s}$. Further, it is assumed that the observational noise ϵ can be modelled by a Gaussian covariance matrix $\mathbf{C_d}$, centered upon the prediction of the forward model. By applying Bayes' theorem [7] [8], it follows that for a specific set of measurements $\Delta\Theta$, the posterior distribution is:

$$\rho(\Delta s|\Delta\Theta_0) \propto exp\left[-1/2(\Delta s - \widehat{\Delta s})^T\widehat{C}^{-1}(\Delta s - \widehat{\Delta s})\right] \tag{5}$$

$$\widehat{\Delta s} = \Delta s_p + \left(\mathbf{M}\mathbf{C}_n^{-1}\mathbf{M} + \mathbf{C}_{\Delta s}^{-1}\right)^{-1}\mathbf{M}^T\mathbf{C}_n^{-1}\left(\Delta\Theta - \mathbf{M}\Delta s_p\right) \tag{6}$$

The most likely solution to (1) is described by $\widehat{\Delta s}$, the mean of the a posteriori distribution. In this study, it is assumed that the noise ϵ is uncorrelated and thus $\mathbf{C}_n$ is the unitary matrix. The *a priori* state of knowledge about $\Delta\Theta$ in (6) is described by the *a priori* mean of the distribution Δs_p and the covariance matrix $\mathbf{C}_{\Delta s}$. This approach of estimating Δs minimizes the expectation of the mean square deviation between the estimation $\widehat{\Delta s}$ and the actual Δs over the assumed probabilistic distribution, which is a reasonable target for regularization. The explicit modelling of the distribution of Δs has a further advantage over the comparably blind Tikhonov regularization: it allows narrowing down the model space, by including prior knowledge of the spatial distribution of SoS into the formulation of the distribution parameters via the covariance matrix $\mathbf{C}_{\Delta s}$. This is achieved by segmenting the B-mode image that is reconstructed in parallel to CUTE into tissue regions within which a correlation of the SoS is expected. Each node in the reconstruction mesh is thus assigned to a segment, and the covariance matrix $\mathbf{C}_{\Delta s}$ is then formed as follows:

$$\mathbf{C}_{\Delta s}(i,j) = \begin{cases} \sigma_A^2 + \sigma_E^2 & \text{if i = j} \\ \sigma_A^2 & \text{if same segment} \\ 0 & \text{else} \end{cases} \tag{7}$$

The allowed variation of the mean SoS over the model space is described by σ_A^2, reflected in the correlation between two nodes within the same segment. To allow also a pixel wise variation of SoS within a segment, σ_E^2 is added to the variation σ_A^2 when i = j. For this study, the variances were chosen to be σ_A^2 = 300 ms^{-1} and σ_E^2 = 30 ms^{-1}. Further, we assumed 1540 ms^{-1} for the *a priori* mean Δs_p.

III. Results and Discussion

Both regularization techniques were compared in phantoms as well as in-vivo, imaging the abdomen of a healthy volunteer accessed form two different scanning locations.

The phantoms were designed to mimic one of our main clinical application goals, namely the diagnosis of fatty liver disease, and are composed of fat mimicking tissue (F: SoS = 1490±5 m/s), muscle mimicking tissue (M: SoS = 1585±5 m/s) and liver mimicking tissue (L1: SoS = 1555±5 m/s, L2: SoS = 1585±5 m/s). As mentioned, in-vivo data contains an increased phase noise compared to phantom data. To mimic this phase noise in the phantom study, synthetic phase noise was added to the phase shift maps. The results are shown in figure 1. For the SP regularization, the B-mode image was segmented as indicated by the dashed red lines in the B-mode images. The SG regularization produced in both phantoms unrealistic SoS variations inside the liver mimicking tissue as well as strong artefacts in the fat mimicking compartments. Further, the spatial distribution of SoS in the muscle mimicking layer deviates from the true SoS distribution. In-vivo, the

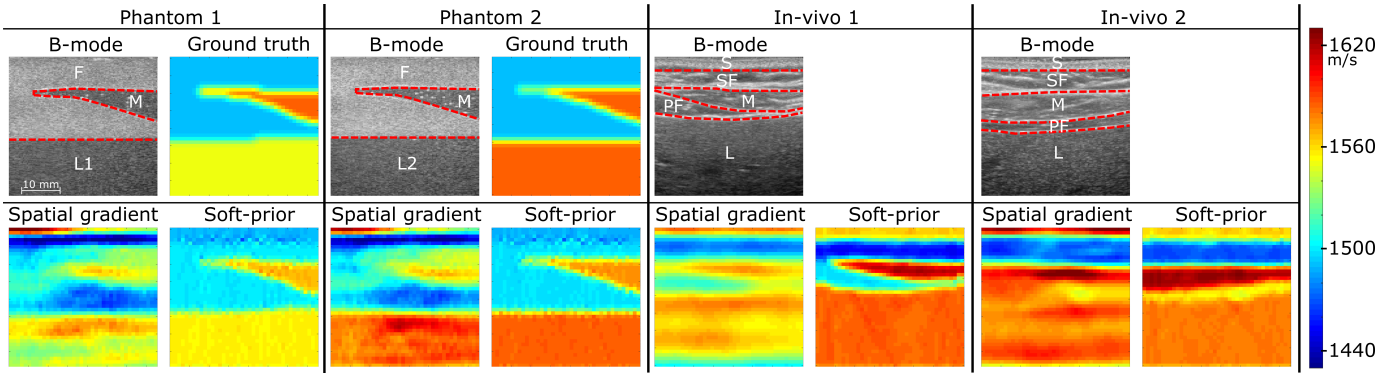

Fig. 1. Phantom and in-vivo results. The top row shows the B-mode images with the segmentation (red dashed lines) and the true SoS distribution of the phantoms. The bottom row shows the SoS images reconstructed with the SG and SP regularization. In-vivo images show images of the abdomen of a volunteer, accessed from different sited (S: Skin, SF: subcutaneous fat, M: rectus abdominis muscle, PF: post peritoneal fat layer, L: liver tissue).

SoS images reconstructed with the SG regularization also show a low axial and lateral resolution of the muscles. Inside the liver, the first in-vivo case shows strong artefacts. Moreover, although a constant SoS inside the liver is expected when imaging the liver from different sides, the SG regularization shows different SoS in the two scenarios. In comparison, the SP regularization shows a distinct improvement of the SoS images. In both phantoms, the SoS of the fat mimicking tissue as well as the liver mimicking tissue agrees well with the true SoS distribution. Only the SoS in the muscle mimicking compartment is in both phantoms slightly underestimated. Also in-vivo, the SP regularization leads to a substantially improved SoS image. Except for the post peritoneal fat layer, the SoS of the other tissue compartments deviates only by a slightley between the two in-vivo images. Furthermore, as expected in healthy liver, the variation of the liver SoS is far below the allowed $\sigma_E^2 = 30\ \mathrm{ms}^{-1}$.

IV. Conclusion

The phantom study revealed that – when phase shift maps are highly contaminated by measurement noise – substantially improved SoS images can be obtained using a SP regularization compared to an SG regularization. The preliminary in-vivo result underlines the great potential of the SP regularization for robust quantitative in-vivo pulse-echo SoS imaging.

References

[1] M. Jaeger, G. Held, S. Peeters, S. Preisser, M. Grünig, and M. Frenz, "Computed ultrasound tomography in echo mode for imaging speed of sound using pulse-echo sonography: proof of principle," Ultrasound in medicine and biology, vol. 41 no. 1 2015, 235-250

[2] P. Stähli, M. Kuriakose, M. Frenz, M. Jaeger, "Forward model for quantitative pulse-echo speed-of-sound imaging," arXiv:1902.10639, 2019.

[3] M. Jaeger and M. Frenz, "Quantitative imaging of speed of sound in echo ultrasonography," IEEE International Ultrasound Symposium - Taipei, 2015.

[4] B. Brooksb, H. Dehghani, B. Pogue, K. Paulsen, "Near-infrared (NIR) tomography breast image reconstruction with a priori structural information from MRI: algorithm development for reconstructing heterogeneities," IEEE Journal of selected topics in quantum electronics, vol. 9 no. 2 2003, 199-209.

[5] M.Althobaiti, H. Vavadi, Q. Zhu, "Diffuse optical tomography reconstruction method using ultrasound images as prior for regularization matrix," Journal of biomedical optics, vol. 22 no. 2 2017, 026002.

[6] T. Loupas, J. Powers, and R. W. Gill, "An axial velocity estimator for ultrasound blood flow imaging, based on a full evaluation of the doppler equation by means of a two-dimensional autocorrelation approach," IEEE transactions on ultrasonics, ferroelectrics, and frequency control, vol. 42 no. 4 1995, 672-688.

[7] A.Tarantola, B. Valette, "Generalized nonlinear inverse problems solved using the least squares criterion," Reviews of Geophysics, vol. 20 no. 2 1982, 219-232.

[8] A. Valentine, M. Sambridge, "Optimal regularization for a class of linear inverse problem," Geophysical Journal International, vol. 215 no. 2 2018, 1003-1023.